Supplementary information

“Regional conditions shape the food-energy-land nexus of low-carbon indoor farming”

Till Weidner[1,2], Aidong Yang[1], Florian Forster[3] and Michael W. Hamm[4]

[1]University of Oxford, Department of Engineering Sciences, Parks Road, Oxford OX1 3PJ, United Kingdom,

[2]ETH Zürich, Institute for Chemical and Bioengineering, Wolfgang-Pauli-Strasse 10, 8093 Zürich, Switherland

[3]Energy Infrastructure Partners, Paradeplatz 5, 8001 Zürich, Switzerland

[4]Michigan State University, Dept. of Community Sustainability, Natural Resources Building, 480 Wilson Road, Rm 312B, East Lansing, MI 48824, United States

1. Further information about methods, parameters and assumptions used in this study

1.1 Composition and micronutrient characteristics of the vegetable basket

Supplementary Table 1: Vegetable basket composition and properties. The average nutrient score determines how much fresh produce would be required per person (50% of RNI equals 376.8 g). The loss combined with the length of the growing period determines any required overproduction to satisfy nutrient needs. The basket properties are derived from the weighted contributions (share in basket) of each crop. The composition is equal in our previous work[1] to allow for a comparison of CEA with open-field farming.

Crop	Share in basket	Max. reported yield (kg m^{-2} $year^{-1}$)	Nutrient score (%RNI 100 g^{-1})	Preservation method	Initial loss
Bell pepper	12%	7.3	17.18	Freeze	15.3%
Broccoli	12%	2.8	17.10	Freeze	10.6%
Lettuce	12%	4.1	11.22	Not applicable	Not applicable
Tomato	40%	12.5	8.64	Canning	19.9%
Spinach	12%	3.6	28.09	Freeze	22.1%
Summer squash	12%	4.9	8.19	Canning	38.1%
Basket	100%	7.6	13.27	Mixed	21.5%

Supplementary Table 2: Selected fresh and processed entries for the vegetables (from Sokolow[2])

Crop code	Crop description (fresh)	Nutrient score	Crop code	Crop description (processed)	Nutrient score
11527	TOMATOES,GREEN,RAW	8.64	11693	TOMATOES,CRUSHED,CANNED	6.92
11821 / 11951	PEPPERS,SWT,RED,RAW PEPPERS,SWEET,YELLOW,RAW	20.69 / 13.68 (17.18)	11917	PEPPERS,SWT,RED,FRZ,CHOPD,UNPREP	17.52 (-15.3%)
11457	SPINACH,RAW	28.099	11463	SPINACH,FRZ,CHOPD OR LEAF,UNPREP	21.88
11477	SQUASH,SMMR,ZUCCHINI,INCL SKN,RAW	8.19	11481	SQUASH,SMMR,ZUCCHINI,ITALIAN STYLE,CND	5.05
11090	BROCCOLI,RAW	17.1	11743	BROCCOLI,FRZ,CHOPD,CKD,BLD, DRND,W/SALT	15.29
11250 / 11252 / 11253 / 11151 / 11152	LETTUCE,BUTTERHEAD (INCL BOSTON&BIBB TYPES),RAW / LETTUCE,ICEBERG (INCL CRISPHEAD TYPES),RAW / LETTUCE,GRN LEAF,RAW / CHICORY,WITLOOF,RAW / CHICORY GREENS,RAW	11.22 (average)		Preservation not realistic	

1.2 Land availability for energy generation

The potential land availability for renewable energy generation has been the subject of many studies with vastly different assumptions. Although they agreed on excluding conservation use and wetland, estimates for relevant land cover categories such as grassland, shrubland and sparsely vegetated land ranged from very low [3,4] to almost 100%[5,6]. A primary reason for this is the differing level of ambition, ranging from current political feasibility[3] to hypothetical or technically realisable[5]. In general, the land availability differed between onshore wind and solar PV, with onshore wind being more favourable in forests[7] and possible in steeper areas[8,9] or higher altitudes[3,5] compared with solar PV. On the other hand, urban areas (mainly rooftops) were considered partly available for solar PV, with reported potentials of around 1-15% of the total urban land[6,10,11].

1.3 Productivity of open-field farming

A host of conditions influence local crop growth, such as summer temperature and precipitation, soil conditions, and plant care factors such as irrigation, drainage and fertilisation[12]. Compared to specific vegetables, wheat and other staple crops have been thoroughly studied. Although the behaviour of specific vegetable cultivars likely differs, this work considers the empirically derived tendencies to be applicable to the vegetable basket as well. The hypothetical yield model thus also draws from studies investigating different staple crops, mainly concerning the effects of precipitation and soil characteristics.

For temperature, a relationship between annual growing degree days (GDD, the annual sum of all average daily temperatures above a specific cardinal temperature) and annual yield[13], as well as the favourability of crop production[14] exists while at the same time, large diurnal temperature extremes negatively affect yield[15]. An adapted model calculates Wang-Engel Degree Days (WEDD) using upper and lower bounds, and an optimum temperature was proposed[16] and tested[17,18]. Still, optimum temperatures differ for the photoperiod and nighttime[19,20] and are observed in practice for vegetable production[21]. This study therefore uses two different temperature correlations depending on the time of day (see Supplementary Figure 1). The average day and night time temperatures of each month were approximated from WorldClim[22] data (minimum and maximum temperatures) via the equations below.

$$T_{day,avg} = (T_{max} - T_{min}) * 0.75 + T_{min}$$

$$T_{night,avg} = (T_{max} - T_{min}) * 0.25 + T_{min}$$

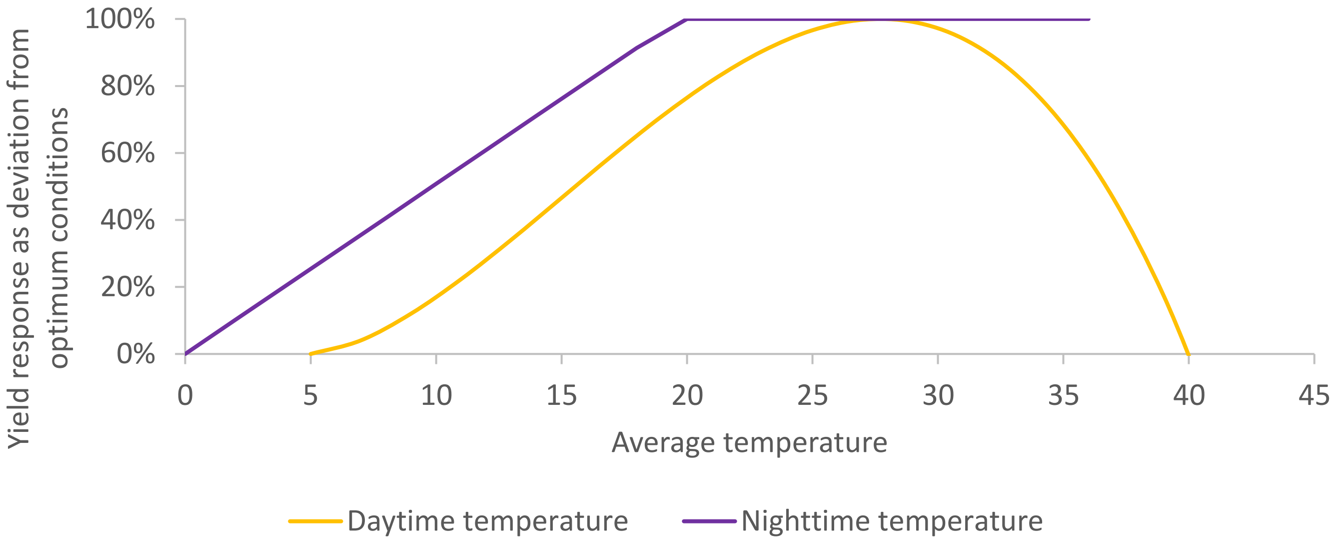

Supplementary Figure 1: Effect of temperature on vegetable growth. The average day and night time temperature are characteristic for each month. The y-axis describes the yield deviation from that of optimum conditions and thus productivity decrease for the specific month. The equations to derive the daytime temperature curve are shown in Aslam et al.[17]

The moisture index, as an indication of the interplay between evapotranspiration and precipitation, has been used to predict the favourability of crop production[14]. Although it is calculated by daily precipitation rates, its value does not describe the seasonal characteristics of rainfall and thus the conditions when most crop production might occur. Optimum amounts of rainfall (around 3.2 inch month^{-1} for wheat) and a strong negative effect on annual yields of staple crops for very high and close-to-zero seasonal precipitation have been observed [12,23]. The shape of this crop response curve seems to depend on crop type, soil type and groundwater conditions[24]. Excessive rainfall, e.g. during monsoon season[25,26] or unusual events[27], have detrimental effects on yields due to soil erosion and plant diseases. Damages during floods make up the majority of harvest loss[28]. Dry spells and droughts also have a negative effect[29]. The impact of excessive rainfall was considered to be more challenging to mitigate than too little rainfall. The yield response to precipitation is shown in Supplementary Figure 2 and derived from the equation below.

$$Yield\ response\ precipitation\ (\%) = \begin{cases} -17 * (EP - 1.7)^2 + 100 & if\ EP < 1.7 \\ -3 * (EP - 5.2)^2 + 100 & if\ EP > 5.2 \\ 100 & else \end{cases}$$

An approximation of soil water storage effects defines effective precipitation (EP, in inch) considering precipitation (P) during the previous months as described in the equation below.

$$EP = P_0 * \frac{2}{3} + P_{-1} * \frac{2}{9} + P_{-2} * \frac{1}{9}$$

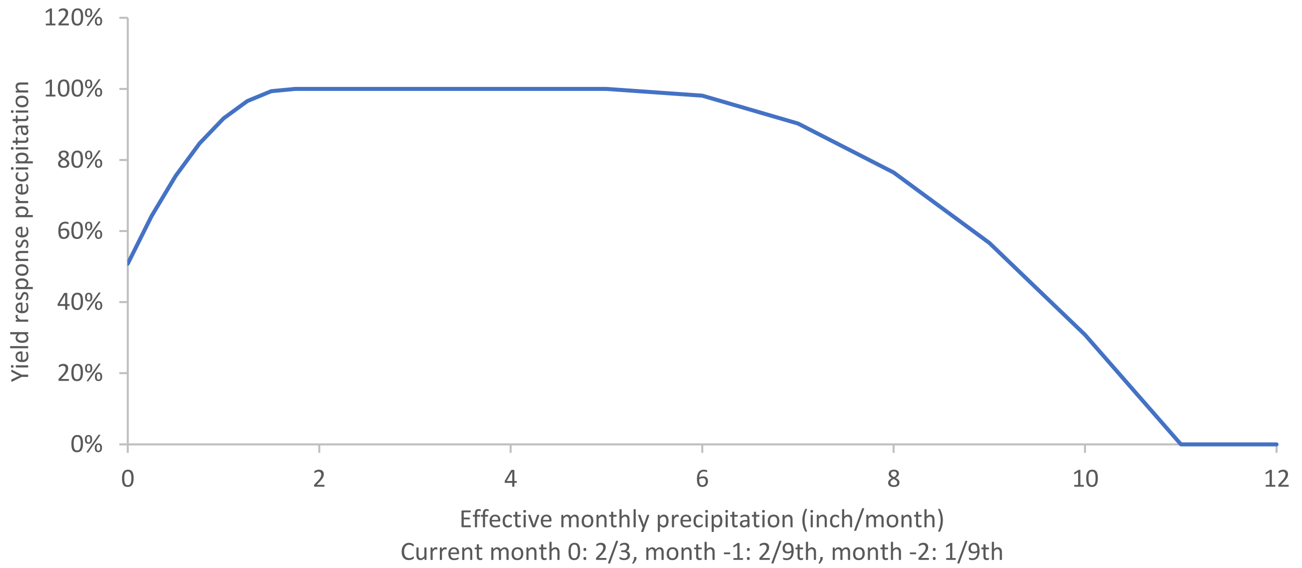

Supplementary Figure 2: Effect of monthly precipitation on vegetable growth. Between 1.7 and 5.2 inch effective monthly precipitation, no negative effect on yields was assumed for the specific month.

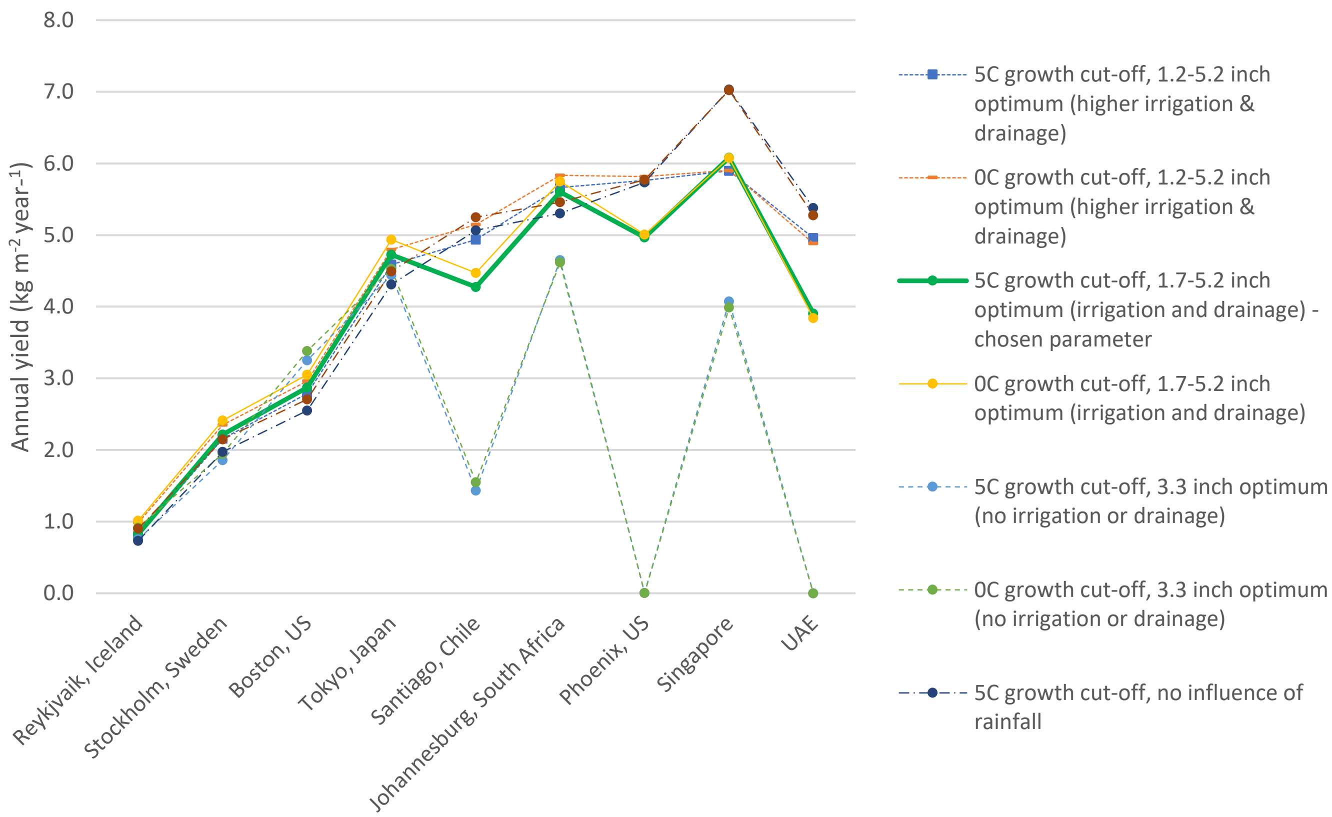

Supplementary Figure 3: Sensitivity analysis for the effect of the effective precipitation influence on annual yields. Excluding the influence of rainfall favours arid (Maricopa County, UAE) and very wet climates (Singapore), while irrigation and drainage ameliorate the impacts of a strong influence of precipitation.

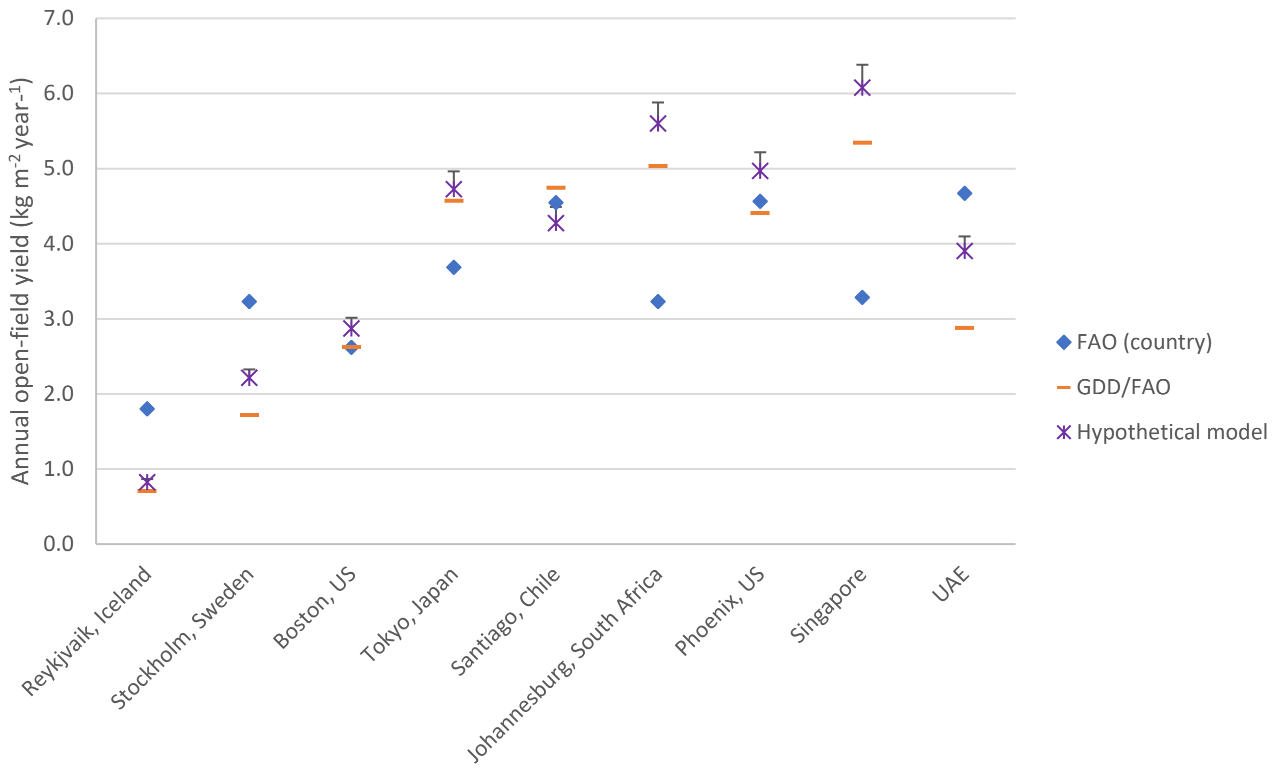

Supplementary Figure 4: Comparison of hypothetical model results for open-field production with reported FAO figures (sometimes influenced by greenhouse production) and growing degree days (GDD) adjusted to FAO figures. The negative error bars for the hypothetical yield model visualise the average yield reductions due to extreme climatic anomalies.

1.4 Length of the growing period and overproduction factor

The local annual yield was adjusted by the overproduction factor (OP). It incorporates the initial processing loss (24.6%), the daily loss (0.1%) and the length of the growing period (LGP) adjusted by the first productive month without harvest, resulting in the length of the harvest period (LHP). The steady consumption of stored food means the average length of the stored food is the total duration divided by 2. If the LGP is below 365, the OP is thus derived via the following steps:

$$percentage\ harvest\ period\ within\ year = LHP\% = \frac{LGP - 30.5}{365}$$

$$percentage\ loss\ of\ stored\ food = Loss\% = \frac{\left(365 - (LGP - 30.5)\right)}{2} * \frac{0.1}{100} + \frac{24.6}{100}$$

$$pood\ to\ be\ produced = annual\ demand * LHP\% + \frac{annual\ demand * (1 - LHP\%)}{1 - Loss\%}$$

$$overproduction\ factor\ (OS) = \frac{food\ to\ be\ produced}{annual\ demand}$$

$$OP = \frac{annual\ demand * LHP\% + \frac{annual\ demand * (1 - LHP\%)}{1 - Loss\%}}{annual\ demand}$$

$$OP = LHP\% + \frac{1 - LHP\%}{1 - Loss\%} = \frac{LGP - 30.5}{365} + \frac{(1 - \frac{LGP - 30.5}{365})}{1 - \left(\frac{\left(365 - (LGP - 30.5)\right)}{2} * \frac{0.1}{100} + \frac{24.6}{100}\right)}$$

1.5 Energy consumption modelling and hourly profiles of CEA facilities

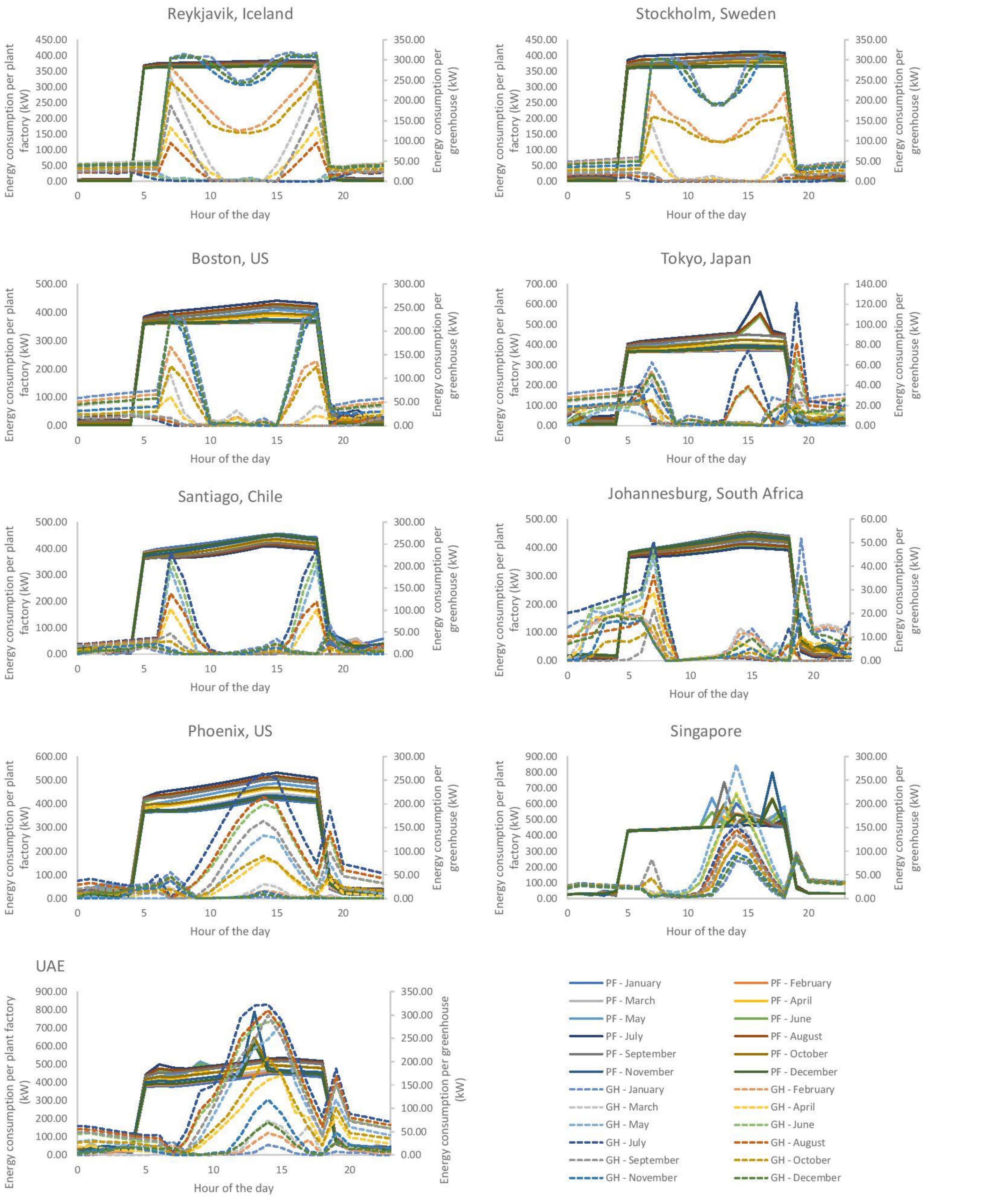

Supplementary Figure 5: Monthly facility load curves for all regions. Note: The units on the two y-axis are different, the primary (left) y-axis describes the energy consumption of plant factories, the secondary y-axis (right) describes the energy consumption of greenhouses.

Less sunny regions (Reykjavik, Stockholm, Boston, Santiago) rely on supplemental lighting in winter and have thus a high load in the morning and evening hours. Very hot regions required substantial mechanical cooling in the summer months when ventilation was insufficient for climate control. The spikes for plant factories in the afternoon hours are due to less efficient cooling (air-to-air cooling was not feasible anymore) when the daytime temperature was at its highest. The early morning and early evening spikes for greenhouses (especially pronounced in Tokyo and Johannesburg) are due to a change in permissible temperature and humidity ranges between day- and night-time settings. It is important to note that those spikes are only moderate, as indicated by the different scaling of the y-axis on each graph (lowest for Tokyo and Johannesburg).

1.6 Renewable electricity: grid optimisation and land-use efficiency

To address the concerns of land impacts of CEA facilities, realistic and fair assumptions need to be made. First, constructing vast quantities of CEA facilities requires additional renewable energy generation potential. Second, the burden on the existing grid should be minimised. Both statements are relevant in a low-carbon world, in which increased electrification and renewable penetration make it substantially more challenging to balance the grid and provide energy security[30]. The implication is that the CEA facilities should be considered prosumers[31] and be powered quasi-independently by renewable energy infrastructure that behaves similar to a micro grid[32]. Simultaneously, this infrastructure would be connected to a regional grid with high renewable penetration and adequate balancing sources, such as biomass, hydropower or nuclear plants. The question is how economics would dictate such a microgrid design with low levels of grid interaction. Several studies have investigated the economic trade-off between the amount of storage (storage days), the share of dispatchable or balancing energy and the overproduction factor (i.e. more energy is produced than required, also called oversizing factor[33], generation factor[34] or overcapacity[35]) for fully or mostly renewable electricity grids. Short-term energy storage is expensive, and installing more renewable generation capacity than required reduces storage requirements exponentially and thus total system costs[35]. At some level of overproduction, these savings become less pronounced[34], with an optimum between 0.3[34] and 1.0[35] storage days and 40[34,36] to 50[35,33] per cent overcapacity. Equally, introducing some level of dispatchable energy, e.g. 5[34,37] to 20[33] per cent, can lead to import-free[33] or significantly cheaper[36] regional grid operations. The amount of dispatchable energy is constrained by the local availability of more steady renewable energy sources, such as hydropower or biomass. Considering local grid imbalances, relying only on local storage alone comes at a high cost but half a day of storage can eliminate most imbalances, even without a regional grid[31].

The land-use efficiencies of renewables follow different principles for onshore wind and solar PV and are expected to improve with time. For wind turbines, the turbine, hub height and blade length are the most decisive parameters[38]. Studies investigating the actual footprint of wind farms range between around 3[10,39,40] to 6[4] MW km^{-2} with a projection for 2030[4] for 8 MW km^{-2}. The direct land footprint of the turbines, including access roads, was considered relatively low, from 1%[39,41] to 5%[38,41], with a lower footprint in areas where wind turbines were co-located with agriculture and existing roads[41]. This study uses a conservative measure of 5% since no double-use of farmland was permitted. For solar PV panels, the panel efficiency and the filling ratio (how much of the land is covered by effective panel area) are most relevant. Panel efficiencies have increased rapidly over the last decades; hence assessments of land-use efficiencies of existing plants with older panels might be on a lower end[4,42] while projections for the future have a wide range, depending on technology[43], with an estimate of 24.4% after 2040[44]. The filling ratio depends on the technology (e.g. axial adjustment and sunlight tracking) and the economic constraints on the land, ranging from 14% for old plants to a feasible maximum of 80%[42]. An average of modern utility-scale plants had a filling ratio of 36.6%[4]. Combined land-use efficiencies (LUE) based on nominal power for existing plants ranged from 17.6 MW km^{-2} for older plants to 25.4 and 36.8 for more recent plants on public and private land, respectively[38]. Since this work considers a more efficient panel (21%) with a nominal capacity per unit area of 209.375 W m^{-2}, the average filling ratio of 36.6% would lead to a land-use efficiency based on nominal power of 76.6 MW km^{-2}.

1.7 Project settings and equipment data for Homer Pro

Location

- Define location based on approximate centre of region and average solar radiation values from ArcGIS for suitable regions (scenario with offshore wind approximately 50 km distance to shore)

Load

- Copied characteristic hourly values each month (scenario with night time operations)
  - Scaled load to number of facilities required for region:

$$\frac{0.318\,\frac{kg}{person*day}*365\;days*regional\;population}{annual\;yield\;per\;facility}$$

- 2.5% timestep fluctuations (random variability)

PV solar

- Type: Panel – SunPower X21-335-BLK with 21% efficiency
- 335 kWp per 1.6 m^2 panel area
- Capital cost 1,000 $ per kW capcity[45]
- O&M cost 0.3% of capital cost (default value)
- Lifetime: 25 years, derating factor: 88%, inverter efficiency: 95%
- No solar tracking

Wind

- Type: Generic 1.5 MW (infinite search space) and Enercon E-115 EP3 E3 4,2 MW (1-10 search space)
- Capital cost 1,350 $ per kW capcity[46,47]
- O&M cost 1% of capital cost (default value)
- Lifetime 20 years, hub height: 80m (1.5 MW), 122 m (4.2 MW)
- Turbine losses (3%), Default power curve

Storage

- Type: Generic 100 kWh Li-ion
- Capital cost 220 $ per kWh capcity[48]
- O&M cost 0.1% of capital cost (default value)
- Roundtrip efficiency 90%
- Lifetime: 15 years, throughput: 300,000 kWh, minimum state of charge 20%

Converter

- Capital cost 300 $ per kWh capacity (default value)
- No O&M cost
- Inverter efficiency 95%, rectifier efficiency 95%
- Lifetime: 15 years

Advanced Grid

- Emissions: 30 g CO_2 kWh^{-1}, 50 \$ $tonne^{-1}$ carbon price (assuming low carbon dispatchable energy)
- Scheduled Rates, Rate Definition:
  - Power price 10 ct kWh
  - Prohibit any grid sales
- Scheduled Rates, Parameter:
  - Maximum net grid purchases: 10% of annual load (scenarios with 0% of the annual load or no restrictions)

Resources

- Scale wind speed at 50m to average value extracted from ArcGIS Pro (see Table SX)

Project

- Economics: 6% nominal discount rate (scenario with 9%), 2% inflation, 25 years project lifetime
- Constraints:
    - Maximum annual capacity shortage to 5% *(explanation: although no serious consequences for CEA facility, stability should be guaranteed)*
    - Operating reserve as percentage of load in current time step: 5% *(explanation: guarantee a degree of stability)*
    - Operating reserve as percentage of annual peak load: 0% *(explanation: no sudden increase in peak load expected)*
    - Operating reserve as a percentage of solar power output: 25% *(explanation: cloud cover forecasted, no significant effect on results)*
    - Operating reserve as a percentage of wind power output: 30% *(explanation: wind speed drops likely, no significant effect on results)*

Results

- Solution with storage and both sources (except for Singapore with PV solar only)

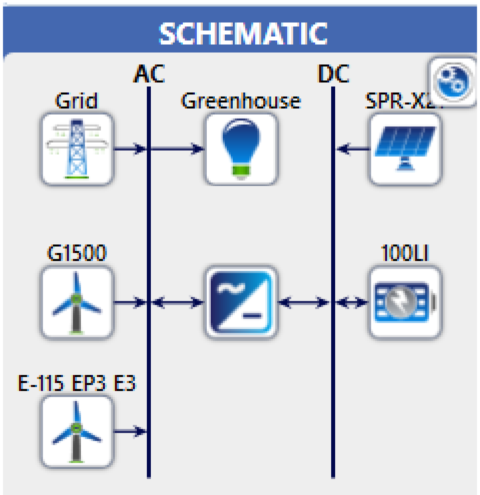

Supplementary Figure 6: Schematic of the Homer Pro microgrid (produced by a screenshot of HomerPro simulation). The optimisation routine selects the least cost set-up for the selected infrastructure items. The grid supply was limited to 10% of the annual load.

1.8 Calculation of per person and relative land-use

Two types of land use considerations were relevant to this study. First, the land use per person for each growing method, considering the direct land use through farming, the required capacity of renewable energy generation capacity (which depends on the energy-efficiency of CEA farming in a particular location and the favourability for renewable energy production as simulated by Homer Pro) and the renewable energy technology-specific land use efficiency (LUE, see SI 1.6). The per-person land use was also influenced by the potential for co-generation of wind and solar PV, determined by the ratio between land suitable for hybrid use and land suitable only for one of the two types. Second, the relative land use characteristics consider the land area available for crop production and energy generation and describe the hypothetical farmland sparing relative to the land requirements for renewable energy generation.

$$solar\ PV\ land\ use\ per\ person = \frac{capacity\ solar\ PV}{LUE_{PV} * regional\ population}$$

$$wind\ land\ use\ per\ person = \frac{capacity\ onshore\ wind}{LUE_{wind} * regional\ population}$$

$$land\ to\ be\ colocated\ per\ person = MIN(\frac{solar\ PV\ land\ use\ per\ person}{0.95}, wind\ land\ use\ per\ person * \frac{land\ suitable\ for\ colocation}{land\ available\ for\ wind\ turbines})$$

The co-location potential was limited either by the amount of land used for solar panels, which can be placed between the wind turbines (accounting for the 5% footprint of turbines) or the share of wind turbines that would be placed on co-location land, assuming equal distribution (determined by the share of land suitable for co-location compared with the land available for wind generation), whichever is smaller.

This effectively considers the setting as if all available land for renewable energy is used for energy generation according to the most economic split recommended by the grid optimisation. For a single renewable energy project with a different demand profile and cost structure, the co-location area could naturally be 100% of the land used, depending on the location. The amount of land suitable for co-location constitutes an overlap of the respective land available for either solar PV or wind and is thus already part of the estimated land for each (e.g. 10 km^2 available for solar PV and wind energy, each with a co-location suitability of 5 km^2 means 15 km^2 is in total available for renewable energy generation).

$$solar\ PV\ (only)\ land\ use\ per\ person = solar\ PV\ land\ use\ per\ person - land\ to\ be\ colocated\ per\ person * (1 - 0.05)$$

$$wind\ (only)\ land\ use\ per\ person = wind\ land\ use\ per\ person - land\ to\ be\ colocated\ per\ person$$

$$additional\ land\ required\ without\ colocation = land\ to\ be\ colocated * 0.95$$

These equations lead to the results illustrated in figure X in the main text.

The relative land use can be assessed in multiple ways. In this study, the relative land use of solar PV and wind energy generation was combined in one number, considering land saving potentials due to co-location. An alternative illustration would be to split the relative land use for both types of renewable energy generation, which was considered less useful here in conveying high-level outcomes comparing the nine regions.

$$Share\ of\ land\ required\ for\ renewable\ energy\ generation = \frac{(solar\ PV\ land\ use\ per\ person + wind\ land\ use\ per\ person) * regional\ population}{land\ available\ for\ wind\ turbines + land\ available\ for\ solar\ PV - land\ suitable\ for\ co\ location * 0.05}$$

The "Renewable energy land abundance relative to the demand for powering CEA" term shown in figure X in the main text is the inverse of the equation above.

The hypothetical farmland sparing was calculated by considering the land not needed anymore for open-field vegetable production and the footprint of the greenhouses.

$$hypothetical\ farmland\ sparing = \frac{Land\ use\ per\ person\ open\ field * regional\ population - [footprint\ growing\ facilities]}{existing\ farmland}$$

A numerical example for the share of land required for renewable energy generation is provided for plant factories in the Reykjavik region in Iceland:

$$solar\ PV\ land\ use\ per\ person = \frac{87489\ kW}{1000\frac{W}{kW} * 76.6\frac{W}{m^2} * 259717} = 4.4\ \frac{m^2}{person}$$

$$wind\ \ land\ use\ per\ person = \frac{150000\ kW}{1000\frac{W}{kW} * 6\frac{W}{m^2} * 259717} = 96.3\ \frac{m^2}{person}$$

$$land\ to\ be\ co\ located = MIN\left(\frac{4.4}{0.95}\ \frac{m^2}{person}, 96.3\ \frac{m^2}{person} * \frac{2954\ km^2}{4207 km^2} = 57.05 \frac{m^2}{person}\right) = 4.4\ \frac{m^2}{person}$$

$$Share\ of\ land\ required\ for\ renewable\ energy\ generation = \frac{\left(4.4\ \frac{m^2}{person} + 96.3\ \frac{m^2}{person}\right) * 259717\ persons}{4207km^2 + 3459\ km^2 - 2954\ km^2 * 0.05} = 0.35\%$$

$$Renewable\ energy\ land\ abundance\ relative\ to\ the\ demand\ for\ powering\ CEA = 288$$

For an alternative scenario, it was assumed that the current farmland was also partly available for energy generation through agriphotovoltaic and wind turbines placed between fields. For agriphotovoltaic, it was assumed that the negative effect on the crops are kept to a minimum by sparsely allocating the solar panels with 1/4th of the land use efficiency previously assumed, hence 25% of farmland was considered available for solar PV. For wind turbines, a clearing of 5% of the project area was required, effectively reducing the agricultural output and thus the land sparing potential of CEA farming. It was assumed that the wind turbines would be distributed among farm and non-farm land according to the ratio between them.

$$Share\ of\ land\ required\ for\ renewable\ energy\ generation\ (alternative\ scenario)$$
$$= \frac{(solar\ PV\ land\ use\ per\ person + wind\ land\ use\ per\ person) * regional\ population}{land\ available\ for\ solar\ PV + land\ available\ for\ wind\ turbines - land\ suitable\ for\ co\ location * 0.05 + agricultural\ land * (1 + 0.25)}$$

$$land\ sparing\ potential\ (alternative\ scenario)$$
$$= \left(Land\ use\ per\ person\ open\ field * regional\ population - [footprint\ growing\ facilities] - wind\ land\ use * 0.05 * \frac{agricultural\ land}{land\ available\ for\ wind\ turbines + agricultural\ land}\right) * \frac{1}{existing\ agricultural\ land}$$

2. Further results

2.1 Tabulated results

Supplementary Table 3: Background information on the regions and intermediate results.

Region	Reykjavik	Stockholm	Boston	Tokyo	Johannes burg	Santiago	Phoenix	Singapore	UAE
Country	Island	Sweden	United States	Japan	South Africa	Chile	United States	Singapore	UAE
Population	259,717	3,556,076	7,503,308	44,012,804	16,916,108	10,378,944	5,369,129	5,870,864	9,318,106
Area (km2)	11,287	38,292	23,809	36,371	39,159	34,610	37,804	697	71,205
Population density (cap km^{-2})	23	93	315	1,210	432	300	142	8,423	131
Climate zone (Koppen)	Cfc	Cfb	Cfa/Dfa/Dfb	Cfa/Cfb/Dfb	Bsh/Cwa/ Cwb	Bsk/Csh/ ET	Bwh	Af	Bwh
Moisture index (Willmot et al.)	0.64	0.01	0.18	0.30	-0.55	-0.64	-0.87	0.38	-0.95
Soil productivity index (1-6)	3.20	4.66	3.53	4.40	4.64	4.97	5	3.05	2.73
GDD (traditional, T_{avg} above 5 C)	460	1338	2199	3297	4064	3804	6077	8012	8370
PGDD adjusted	817	2027	2785	4477	5402	5067	5743	7841	6106
Length of growing season (days)	183	183	183	336	365	365	275	365	214
Overproduction required	49%	49%	49%	7%	0%	0%	19%	0%	37%
Average annual windspeed ($m\ s^{-1}$)	7.31	4.25	4.44	5.16	5.03	2.86	4.43	4.21	4.28
Average annual solar radiation ($kWh\ m^{-2}\ day^{-1}$)	2.09	2.75	3.70	3.78	5.53	5.56	5.35	4.56	5.91
Fresh vegetable supply target (1000 tonnes)	35.7	489.1	1,031.9	6,053.2	1,427.4	2,326.5	738.4	807.4	1,281.5
Local yield factor	0.08	0.23	0.29	0.48	0.44	0.57	0.51	0.62	0.40
Primary load per plant factory ($MWh\ year^{-1}$)	5,697	5,882	6,021	6,426	6,492	6,436	6,993	7,578	7,541
Facility yield plant factory ($kg\ year^{-1}$)	366,007	362,871	361,784	358,553	358,128	357,461	356,644	348,150	353,476
Number of plant factories required	98	1,348	2,852	16,882	6,496	3,993	2,070	2,319	3,626
Primary load per greenhouse ($MWh\ year^{-1}$)	683.7	539.6	288.2	129.3	69.7	173.6	306.3	377.0	526.5
Facility yield greenhouse ($kg\ year^{-1}$)	75,131	71,643	68,148	61,060	60,450	61,784	59,082	53,788	59,803
Number of greenhouses required	475.43	6,827	15,143	99,135	23,614	37,655	12,498	15,011	21,429
Regional electricity consumption ($TWh\ year^{-1}$)	13.47	47.01	88.45	328.40	59.07	39.75	63.29	47.69	113.20

Supplementary Table 4: Results from grid optimisation – Plant Factories.

Region	Reykjavik	Stockholm	Boston	Tokyo	Johannes burg	Santiago	Phoenix	Singapore	UAE
Country	Island	Sweden	United States	Japan	South Africa	Chile	United States	Singapore	UAE
NPV per facility (million USD)	654	12,373	26,530	210,377	53,115	32,875	19,001	33,405	32,239
COE ($\$\ kWh^{-1}$)	0.075	0.099	0.098	0.128	0.080	0.081	0.083	0.121	0.075

PV solar capacity (MW)	87	3,201	10,125	126,364	18,098	10,993	6,794	18,477	10,159
Onshore wind capacity (MW)	150	2,494	2,729	206	4,797	3,397	1,479	-	3,661
Day equivalent storage requirements	0.30	0.33	0.4	0.5	0.32	0.32	0.37	0.5	0.28
Share PV solar of load (excl. grid)	8.5%	30.6%	66.10%	99.70%	74.5%	71.4%	79.4%	100.00%	65.4%
Over-production factor[1]	45.9%	47.1%	24.10%	69.90%	12.2%	18.3%	14.2%	54.10%	14.5%
Loading factor wind	58.2%	37.1%	30.2%	28.4%	28.8%	29.2%	26.3%	20.6%	33.8%
Loading factor PV solar	9.0%	12.7%	15.9%	16.0%	22.3%	22.5%	22.1%	16.7%	23.0%

1 Due to grid supply restrictions, 10% of annual load

Supplementary Table 5: Results from grid optimisation – Greenhouses.

Region	**Reykjavik**	**Stockholm**	**Boston**	**Tokyo**	**Johannes burg**	**Santiago**	**Phoenix**	**Singapore**	**UAE**
Country	Island	Sweden	United States	Japan	South Africa	Chile	United States	Singapore	UAE
NPV per facility (million USD)	438	12,209	14,183	44,591	6,638	16,487	9,947	13,020	20,934
COE ($ kWh^{-1})	0.086	0.210	0.206	0.221	0.157	0.261	0.165	0.146	0.118
PV solar capacity (MW)	1	1	1,892	17,737	1,392	3,150	4,264	6,183	8,312
Onshore wind capacity (MW)	154	3,874	2,780	66	608	2,710	836	-	1,981
Day equivalent storage requirements	0.26	1.08	1.2	1.63	1.18	1.54	0.60	0.78	0.40
Share PV solar of load (excl. grid)	0.1%	0.0%	26.30%	99.30%	63.9%	47.2%	81.0%	100.00%	74.0%
Over-production factor[1]	135.7%	241.6%	129.00%	95.10%	58.4%	227.7%	165.6%	60.10%	100.5%

1 Due to grid supply restrictions, 10% of annual load

Supplementary Table 6: Scenario analysis for grid optimisation – changing the load time, location and discount rate.

Region	**Reykjavik**	**Stockholm**	**Boston**	**Stock-holm**	**Tokyo**	**Singapore**	**Reykjavik**	**Reykjavik**	**UAE**	**UAE**
Scenario	Night time operation[1]	Night time operation[1]	Night time operation[1]	Off-shore wind[2]	Offshore wind[2]	Offshore wind[2]	9% discount rate (GH)	9% discount rate (PF)	9% discount rate (GH)	9% discount rate (PF)
Primary load per plant factory (MWh $year^{-1}$)	5,720	5,850	5,983	5,882	6,426	7,578	5,697	5,697	7,541	7,541
NPV per facility (million USD)	800	17,302	39,437	11,188	104,252	60,230	383	590	19,441	29,300
COE ($ kWh^{-1})	0.091	0.139	0.147	0.090	0.063	0.218	0.100	0.090	0.146	0.091
PV solar capacity (MW)	-	2,318	7,250	-	-	-	-	63	8,140	10,528
Onshore wind capacity (MW)	184	2,937	5,127	2,463	29,214	21,630	144	157	2,033	3,134
Day equivalent storage requirements	0.97	0.60	1.09	0.62	0.25	0.92	0.27	0.33	0.41	0.30
Share PV solar of load (excl. grid)	21.3%	0.0%	42.6%	0.0%	0.0%	0.0%	100.0%	6.0%	73.1%	69.5%
Over-production factor[1]	53.7%	65.5%	38.7%	59.3%	46.0%	180.7%	125.9%	48.1%	98.7%	11.5%

Loading factor wind (offshore)	-	-	-	58.2%	59.9%	26.0%	-	-	-	-

1 Choice of location due to limited seasonal sunshine

2 Choice of location due to good connection to open sea and existing wind farms

Supplementary Table 7: Scenario analysis for grid optimisation – modulating the grid contribution.

Region	**Reykjavik**	**Reykjavik**	**UAE**	**UAE**	**Reykjavik**	**Reykjavik**	**UAE**	**UAE**
Scenario	No grid access (PF)	No grid restrictions (PF)	No grid access (PF)	No grid restrictions (PF)	No grid access (GH)	No grid restrictions (GH)	No grid access (GH)	No grid restrictions (GH)
NPV per facility (million USD)	792	510	33,885	29,939	583	353	23,702	15,642
COE ($/kWh)	0.094	0.058	0.082	0.069	0.118	0.069	0.139	0.088
PV solar capacity (MW)	151	-	13,350	7,530	0	-	11,131	2,474
Onshore wind capacity (MW)	175	-	3,345	2,853	176	112	1,023	1,281
Day equivalent storage requirements	0.51	0.00	0.43	0.01	0.69	-	0.68	-
Share PV solar of load (excl. grid)	12.0%	0.0%	73.1%	64.2%	0.2%	0.0%	88.1%	56.8%
Over-production factor[1]	85.8%	7.6%	39.5%	-13.6%	187.5%	75.7%	135.6%	-22.2%

Supplementary Table 8: Scenario analysis for grid optimisation – land unconstrained renewable energy provision.

Region	**Singapore**	**Singapore**	**Tokyo**	**Tokyo**	**Boston**	**Boston**
Scenario	No constraints on wind - GH	No constraints on wind - PF	No constraints on wind - GH	No constraints on wind - PF	No constraints on wind - PF	No constraints on wind - GH
NPV per facility (million USD)	12,132	29,341	34,542	170,495	26,067	13,970
COE ($\$\ \text{kWh}^{-1}$)	0.136	0.106	0.171	0.102	0.096	0.203
PV solar capacity (MW)	4,547	11,715	7,426	58,829	8,147	1,322
Onshore wind capacity (MW)	1,090	3,159	5,087	26,317	3,994	3,267
Day equivalent storage requirements	0.61	0.4	1.05	0.33	0.36	1.12
Share PV solar of load (excl. grid)	22.20%	75.00%	45.10%	55.70%	51.70%	17.50%
Over-production factor[1]	55.20%	30.20%	79.80%	39.40%	27.60%	140.50%

Supplementary Table 9: Combined land use considering co-location, all numbers in m^2 $capita^{-1}$.

Region / Country	**Reykjavik**	**Stockholm**	**Boston**	**Tokyo**	**Johannes burg**	**Santiago**	**Phoenix**	**Singapore**	**UAE**
Land use category	Island	Sweden	United States	Japan	South Africa	Chile	United States	Singapore	UAE
Open-field direct	303.6	113.1	87.2	38.0	40.5	30.9	40.2	28.5	58.9
Greenhouse growing direct	4.58	4.80	5.05	5.63	5.69	5.57	5.82	6.39	5.75
Greenhouse solar only	0.0	0.0	0.0	5.2	0.0	0.0	0.0	13.7	0.0
Greenhouse co-located land	0.1	0.0	3.5	0.0	4.2	1.1	10.9	0.0	12.3
Greenhouse wind only	98.7	181.6	58.3	0.2	39.4	4.9	15.1	0.0	23.2
Greenhouse savings due to co-location	0.1	0.0	3.3	0.0	4.0	1.1	10.4	0.0	11.6

Plant factory growing	0.47	0.47	0.48	0.48	0.48	0.48	0.48	0.49	0.49
Plant factory solar only	0.0	5.1	13.6	37.4	0.0	0.0	0.0	41.1	0.0
Plant factory co-located land	4.6	6.6	4.0	0.1	14.5	14.7	17.4	0.0	15.0
Plant factory wind only	91.6	110.2	56.6	0.7	40.0	32.6	28.5	0.0	50.5
Plant factory savings due to co-location	4.4	6.3	3.8	0.0	13.8	14.0	16.5	0.0	14.2

Supplementary Table 10: Relative land use considering co-location, greenhouses are allocated on farmland.

Region / Country	**Reykjavik**	**Stockholm**	**Boston**	**Tokyo**	**Johannes burg**	**Santiago**	**Phoenix**	**Singapore**	**UAE**
Land use category	Island	Sweden	United States	Japan	South Africa	Chile	United States	Singapore	UAE
Share farmland saved (GH)	25.8%	5.3%	41.2%	44.8%	5.1%	7.8%	7.9%	6482.1%	100.0%
Share direct farmland needed (GH)	0.39%	0.35%	2.84%	7.93%	0.89%	1.74%	1.38%	1876.4%	10.81%
Share farmland saved (PF)	26.1%	8.3%	48.7%	52.9%	6.3%	9.5%	9.4%	8213.6%	110.0%
Share direct farmland needed (PF)	0.04%	0.03%	0.27%	0.68%	0.08%	0.15%	0.11%	144.95%	0.91%
Share available land for energy combined required (GH)	0.4%	47.7%	76.8%	76.6%	3.1%	1.3%	1.4%	668.1%	0.8%
Share available land for energy combined required (PF)	0.35%	32.9%	85.7%	263.1%	3.9%	6.2%	2.1%	1362.7%	1.2%
Share available solar PV land (GH)	0.00%	0.0%	11.0%	40.3%	0.3%	0.2%	0.4%	456.0%	0.3%
Share available wind land (GH)	0.61%	52.2%	100.0%	16.7%	7.6%	1.8%	5.5%	-	1.1%
Share available solar PV land (PF)	0.03%	26.5%	59.1%	287.3%	1.2%	2.1%	0.7%	1362.7%	0.4%
Share available wind land (PF)	0.59%	33.6%	98.3%	51.9%	9.5%	14.4%	9.8%	-	2.0%

Supplementary Table 11: Current carbon intensity of electricity consumption and projected carbon intensity of CEA produce for current grid conditions and regional renewable electricity supply (solar PV utility and onshore wind emissions intensity values according to [49]). The carbon intensity of produce for regional renewable electricity supply includes the overgeneration determined in this work but excludes the grid share (10%).

Region / Country	**Reykjavik**	**Stockholm**	**Boston**	**Tokyo**	**Johannes burg**	**Santiago**	**Phoenix**	**Singapore**	**UAE**
Carbon intensity of national electricity consumption (g $CO2_{eq}$/kWh)	9.8 (Iceland, 2019) [50]	12 (2018)[51]	333 (MA, 2019)[51]	506 (Japan, 2018)[51]	928 (South Africa, 2018)[51]	180 (Chile, 2018)[52]	441 (Arizona, 2018)[51]	419 (2018)[51]	426 (2018)[51]
Carbon intensity of GH produce, current grid (kg $CO2_{eq}$/kg crop)	0.08	0.09	1.30	0.96	0.93	0.44	1.89	2.71	3.27
Carbon intensity of PF produce, current grid (kg $CO2_{eq}$/kg crop)	0.15	0.19	5.54	9.07	16.85	3.23	8.65	9.77	9.09
Carbon intensity of GH produce, renewable grid (kg $CO2_{eq}$/kg crop)	0.22	0.27	0.16	0.18	0.05	0.23	0.47	0.46	0.59

Carbon intensity of PF produce, renewable grid (kg $CO2_{eq}$/kg crop)	0.32	0.53	0.64	1.46	0.79	0.80	0.90	1.61	0.86

Supplementary Table 12: Region specific takeaways derived from the relative land use and renewable energy assessment.

Region	Recommendations
Reykjavik	A vast amount of resources (land, geothermal) are available for renewable energy production and open-field growing is challenging due to its extreme climate. Hence, a clear recommendation for CEA, irrespective of the growing method and the extent of the scale-up.
Stockholm	Very limited land available for onshore wind and solar-based renewable energy production compared with existing farmland. Nevertheless, current electricity grid is low-carbon and additional offshore wind capacity can be installed. Thus, shifting some vegetable production to plant factories can increase resilience without significant additional CO_2 or land use burdens. Additionally, localising open-field vegetable production would also be sensible as it requires less than 10% of the existing farmland.
Boston	The larger Boston regions features comparatively little land for renewable energy production or open-field farming. Land savings for CEA facilities being supplied with onshore wind (which is more economic than solar PV) are rather low. The considerable rooftop area in the regions could be used for solar PV to operate some CEA facilities but a full scale-up is not favourable. States with more available land and better renewable resource conditions (e.g. in the South and South-West of the US) could provide low-carbon electricity and make CEA more favourable if transmission is economical.
Tokyo	Much of the land in the Greater Tokyo Region is already used or inaccessible (surrounding mountains), there is thus limited potential for renewable energy generation. The dwindling contributions of nuclear to the electricity mix make current CEA production less favourable. Nevertheless, additional offshore wind capacity or solar PV on rooftops can supply low-carbon electricity for some CEA farms, with greenhouses being especially favourable.
Santiago	The region around Santiago features a high potential to fully supply vegetables through open-field farming. Although windy regions exist close to the shore, the land footprint is higher and thus CEA is not particulary beckoning (both greenhouses and plant factories). However, resilience considerations might justify some CEA.
Johannesburg	The climate in the Johannesburg region and the large amount of farmland is conducive to open-field vegetable production. At the same time, greenhouses can be operated with very little energy and thus land requirements. If economics are favourable, localising vegetable supply with greenhouses can secure self-sufficiency and free-up land for other uses. Plant facotires are less sensible in this region.
Phoenix	The land use of growing methods is comparable in Pheonix. As sufficient land for both, renewable energy production and open-field growing is available, no clear recommendation can be given and all growing methods can contribute to nutritional self-sufficiency. Economics, water use and resilience might play a more pronounced role.
Singapore	Singapore is a special case as there is no rural hinterland. The few dedicated zones for agriculture ideally focus on productivity and greenhouses are particularly favourable. Further assessments about rooftop potentials are required; if greenhouses or open-field gardens can be built on them, it might be more sensible than merely installing solar PV panels to power plant factories. If not, some plant factories, supplied by solar PV from rooftops and some imported low-carbon electricity, could help achieve self-sufficiency targets.
UAE	A clear recommendation for CEA can be given for UAE. Limited farmland and extensive land available for utility scale solar PV plants allow UAE to fully scale-up CEA in either greenhouses (slightly favoured) or plant factories while saving scarce water.

2.2. Cost of energy and storage requirements

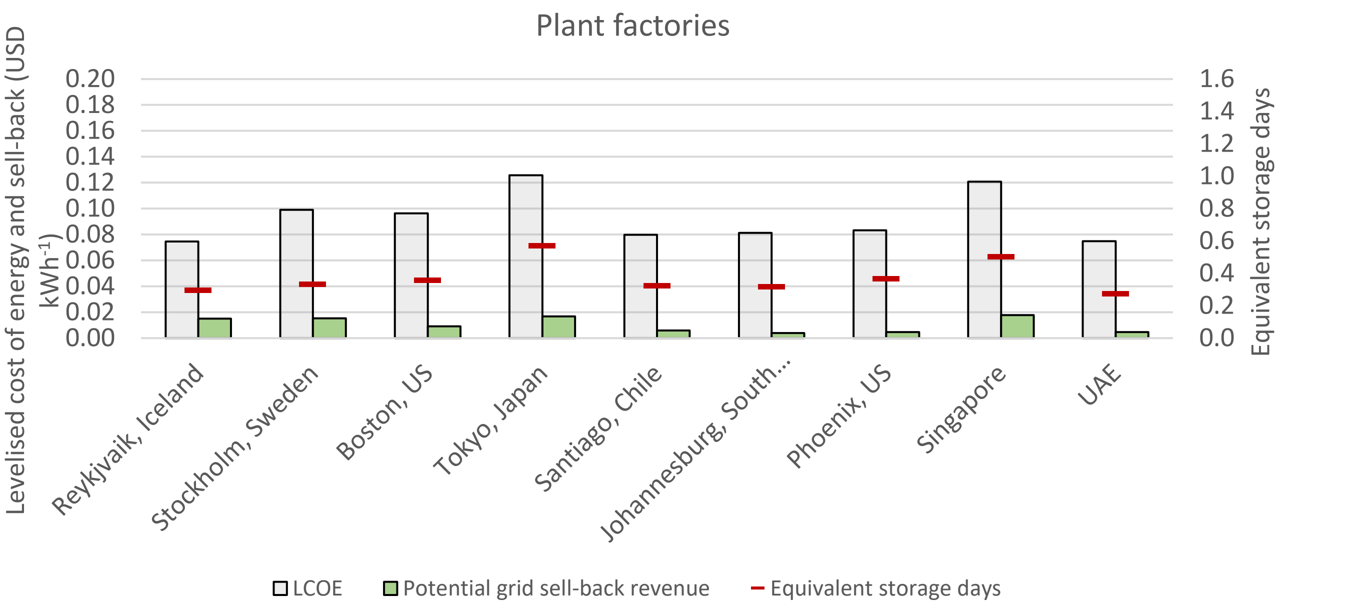

Supplementary Figure 7: Results from the grid cost optimisation with Homer Pro for greenhouses; the levelised cost of energy (LCOE) indicates the cost per unit energy considering infrastructure, project duration and output. The potential grid sell-back revenue assumes that all overgeneration can be utilised regionally and is discounted with the same rate as the LCOE. The equivalent storage days relate the storage capacity with the daily electricity generation. A value of 1 indicates that the average generation of 1 full day can be stored in a battery. Due to the high cost of energy storage, this parameter had a strong influence on the LCOE.

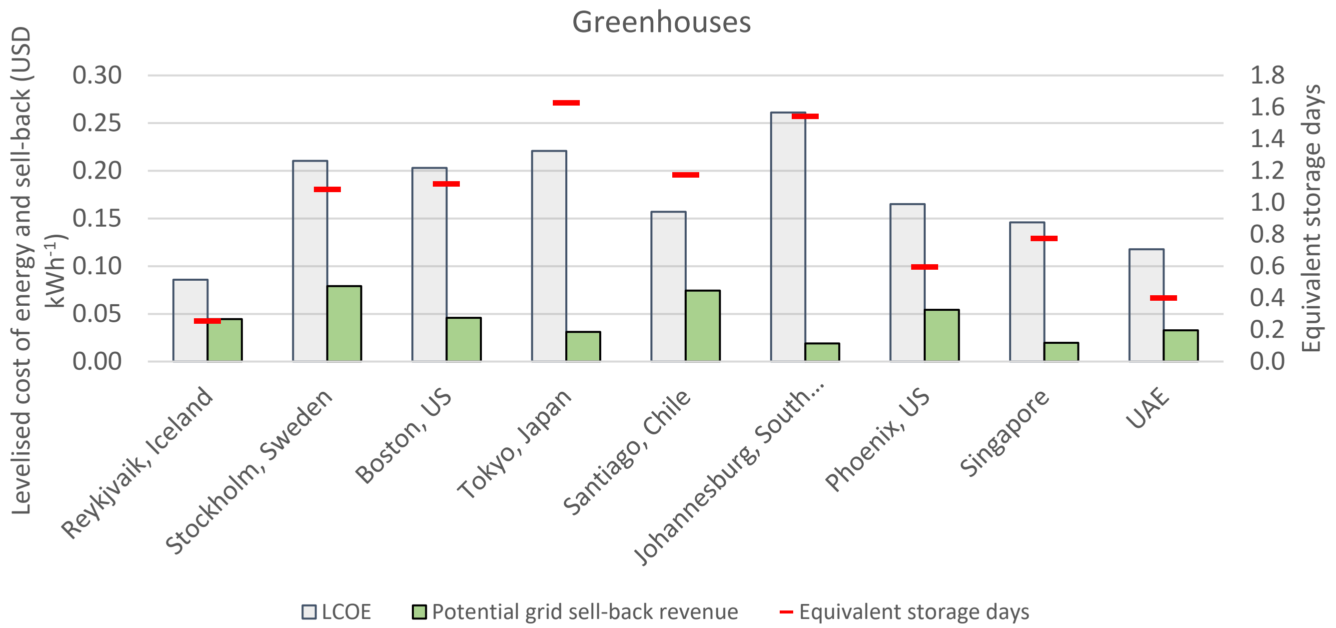

Supplementary Figure 8: Results from the grid cost optimisation with Homer Pro for plant factoriess; the levelised cost of energy (LCOE) indicates the cost per unit energy considering infrastructure, project duration and output. The potential grid sell-back revenue assumes that all overgeneration can be utilised regionally and is discounted with the same rate as the LCOE. The equivalent storage days relate the storage capacity with the daily electricity generation. A value of 1 indicates that the average generation of 1 full day can be stored in a battery. Due to the high cost of energy storage, this parameter had a strong influence on the LCOE.

The LCOE for PFs is significantly correlated with the need for storage (Supplementary Figure 8), which was higher when relying on solar PV only. Less optimal wind conditions (e.g. Stockholm and Boston) also increased the LCOE. Night-time operations in PFs and offshore wind scenarios (Supplementary Table 6) always lead to higher costs and installed capacities due to the lack of otherwise load-matching solar PV, even in windy locations such as Reykjavik.

For GHs, the LCOE (Supplementary Figure 7) was highest for locations with strong fluctuations in the daily load curves (e.g. Johannesburg and Tokyo) and lowest for locations with favourable renewable energy sources (e.g. wind in Reykjavik and solar PV in UAE).

The sensitivity of results to a higher discount rate was little (Supplementary Table 6). A stronger sensitivity was observed for grid interaction limits (Supplementary Table 7): if they were removed, the LCOE dropped by up to 25% and the overgeneration ratio was negative (implying a high grid contribution), while having no access to dispatchable grid energy increased the LCOE by up to 37% and the overgeneration ratio by up to 172% (with corresponding implications on land use). The majority of overgeneration in GHs occurred during winter midday in cold and temperate regions, in summer of cold locations (no lighting required), or in winter of hot locations (no cooling required). These spikes deserve special attention when considering regional demand balance between CAE and other sectors.

2.3. Alternative scenarios for combined land use and influencing factors

If Boston, Tokyo and Singapore were also able to employ wind to achieve a lower energy cost, PFs would require significantly more land than open-field farming (Supplementary Figure 9). The combined land use for plant factories differs quite significantly between the regions. The main driver for this is the share between solar PV and wind but

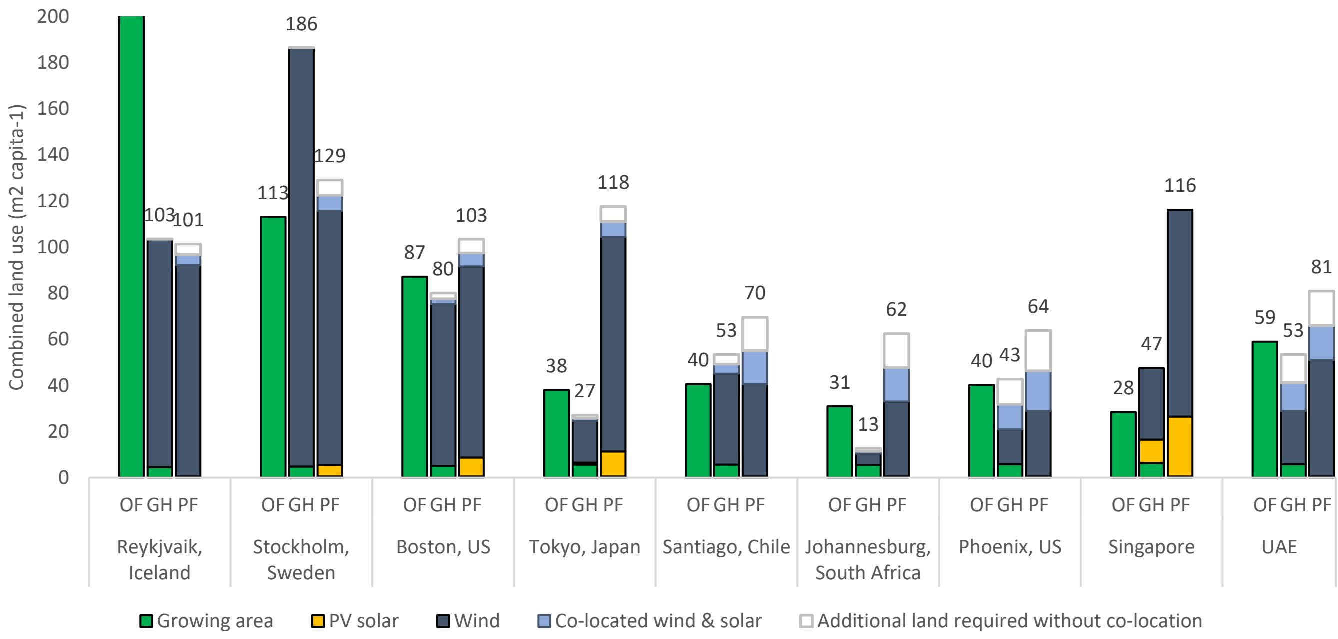

Supplementary Figure 9: Combined land use efficiency of the three growing techniques without land restrictions on wind energy in Singapore and Tokyo. The land required to generate the required electricity is included and hybrid land use is preferred.

also the overgeneration as a result from daily and seasonal mismatch between demand and supply, which was mitigated by an economic trade-off between energy storage and installing more capacity. The total required capacity was influenced, in turn, by a) fluctuations of load or energy demand, (e.g. when air-to-air cooling was not feasible in the afternoon hours in Tokyo, Singapore and UAE), b) an unfavourable complementarity between seasonal characteristics of solar radiation and wind power (e.g. very low windspeed in some seasons in Singapore) and c) the energy demand per facility (cooling was more energy-intensive in hot climates). The seasonal non-complementarity for a region between solar PV and wind was calculated as shown below, using monthly and annual average values of global horizontal irradiation (GHI) and wind power, calculated using the power curve of the turbines and the wind speed.

$$\left[\sum_{i=1}^{12} ABS\left(\frac{x_{GHI,i} - AVG_{GHI}}{AVG_{GHI}} + \frac{x_{wind\ power,i} - AVG_{wind\ power}}{AVG_{wind\ power}}\right)\right] * \frac{1}{12}$$

Supplementary Figure 10 shows the relative values for each of these parameters compared with the maximum value of all regions. Supplementary Figure 11 visualises the combined land required for increased yields in CEA facilities (50% more in GHs, up from around 30 to 35 kg m^{-2} for the basket, and 75% more in PFs, up from around 40 kg m^{-2} based on our previous work[1]), which suggests that advances in science and growing practices have a significant impact on the comparative results. A re-calculation of the combined land use as if all excess energy could be utilised within the region for other purposes is presented in Figure S15, implying a reduced hypothetical land allocation of the solar and wind farms to CEA production. In that case, the land use of GHs (which remains to be the lowest) is reduced more than that of the PF since the fluctuating load profile is more relevant for the former. This means that finding a regional use for excess energy is more relevant and impactful for GHs, while PFs would now require less land overall than open-field farming in all locations except Johannesburg. The sensitivity of results to the land-use efficiency of solar panels is shown in Supplementary Figure 12, indicating that a threshold panel density exists to equalise the combined land use for open-field farming and PFs, except in Johannesburg and UAE (where PF always requires more or less land than open-field farming, respectively).

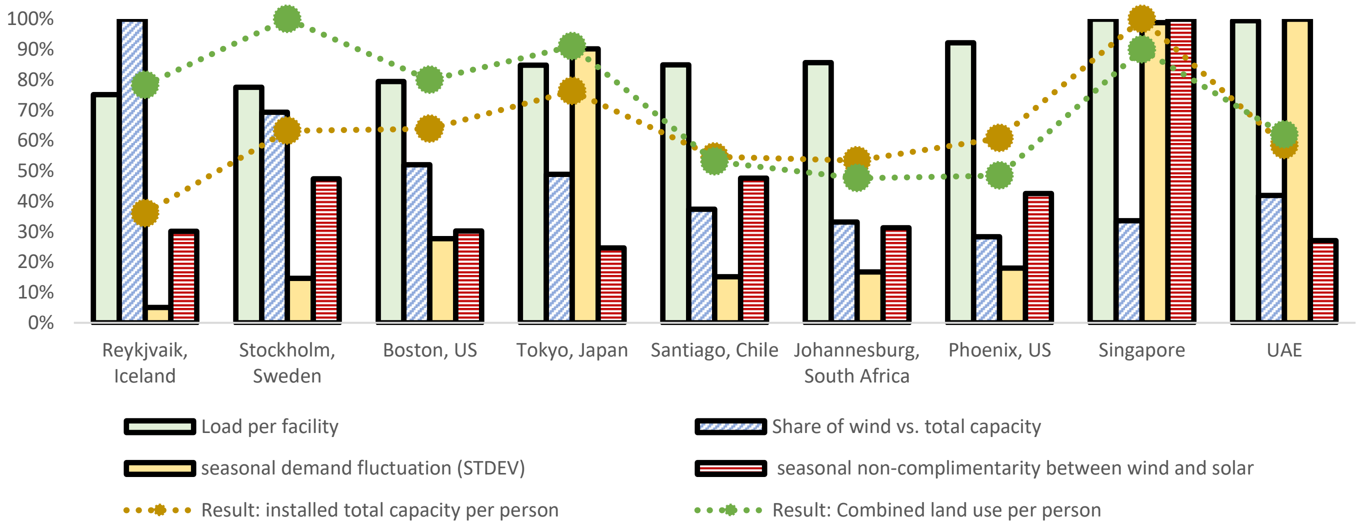

Supplementary Figure 10: Overview of aspects influencing the combined land use per person of PFs. All values are displayed relative to the maximum value in a region for the specific category. The dotted lines between the regions are only for trend visualisation. A low value for seasonal wind and solar mismatch describes a favourable seasonal match.

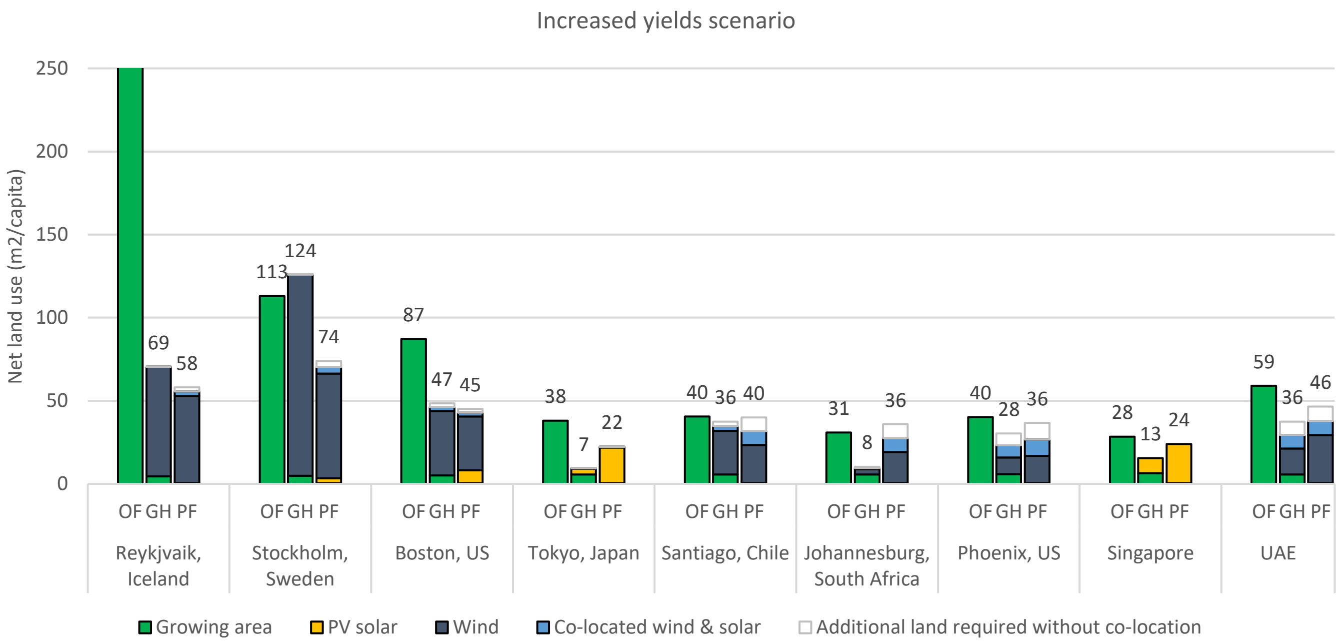

Supplementary Figure 11: Combined land use efficiency of the three growing techniques, considering a yield increase of 50% in greenhouses and 75% in plant factories. The land required to generate the required electricity is included and hybrid land use is preferred. The value for open field farming in Iceland is 305.1 m^2 $capita^{-1}$.

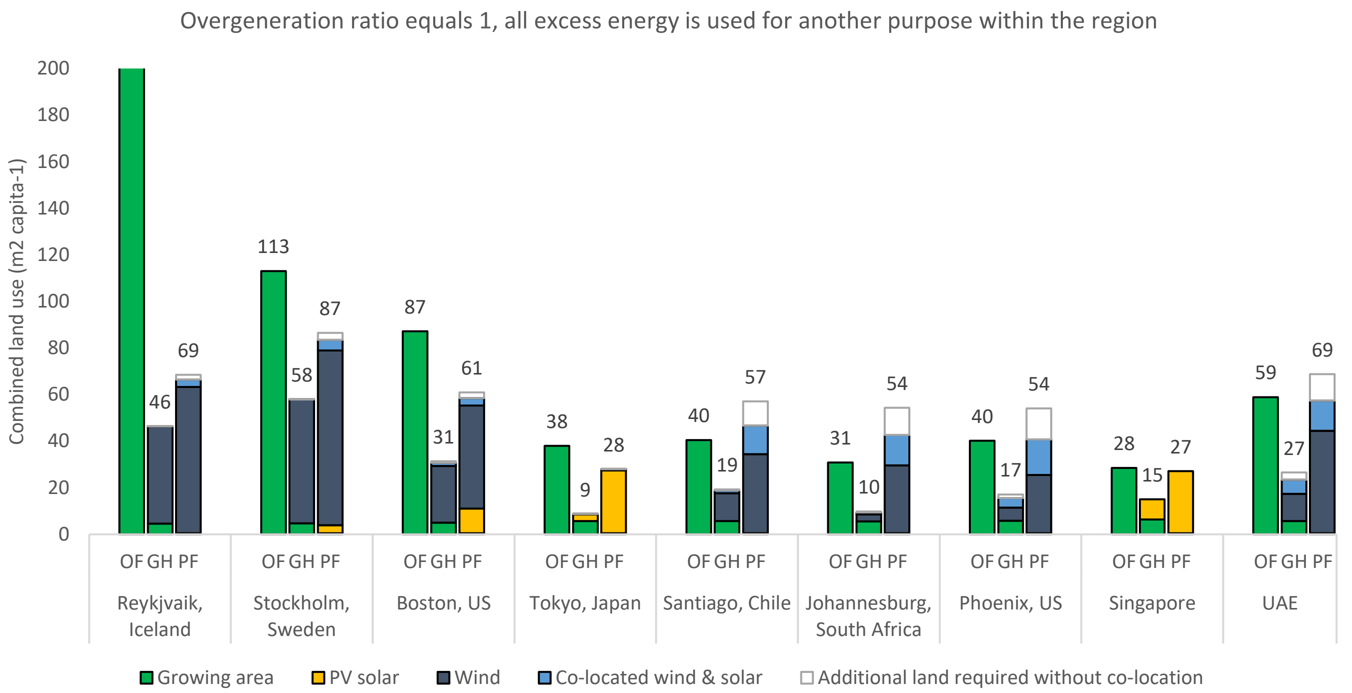

Supplementary Figure 12: Combined land use efficiency of the three growing techniques, considering an overproduction factor of 1 (i.e. electricity generation equals consumption). The land required to generate the required electricity is included and hybrid land use is preferred. The value for open field farming in Iceland is 305.1 m^2 $capita^{-1}$.

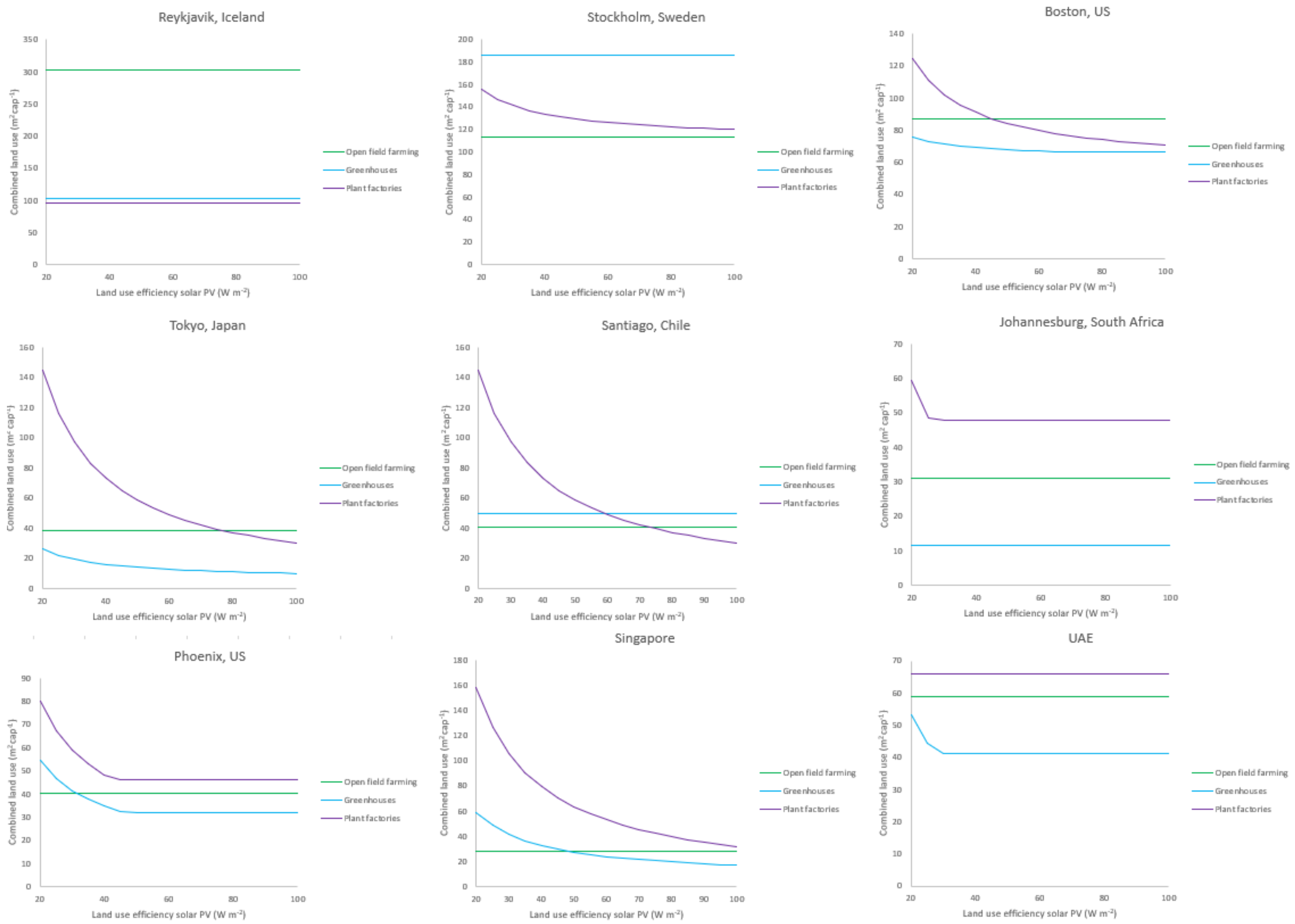

Supplementary Figure 13: Sensitivity of combined land use to the land use efficiency of solar PV.

2.4. Alternative scenarios for the relative land use

Supplementary Figure 14: Relative land use requirements of the CEA practices by the type of land available for either solar PV or wind turbines. The bubble size depicts the net land use per person subtracted with savings of co-locating solar PV and wind. The dashed-line circle is for greenhouses and the solid-line circle is for plant factories.

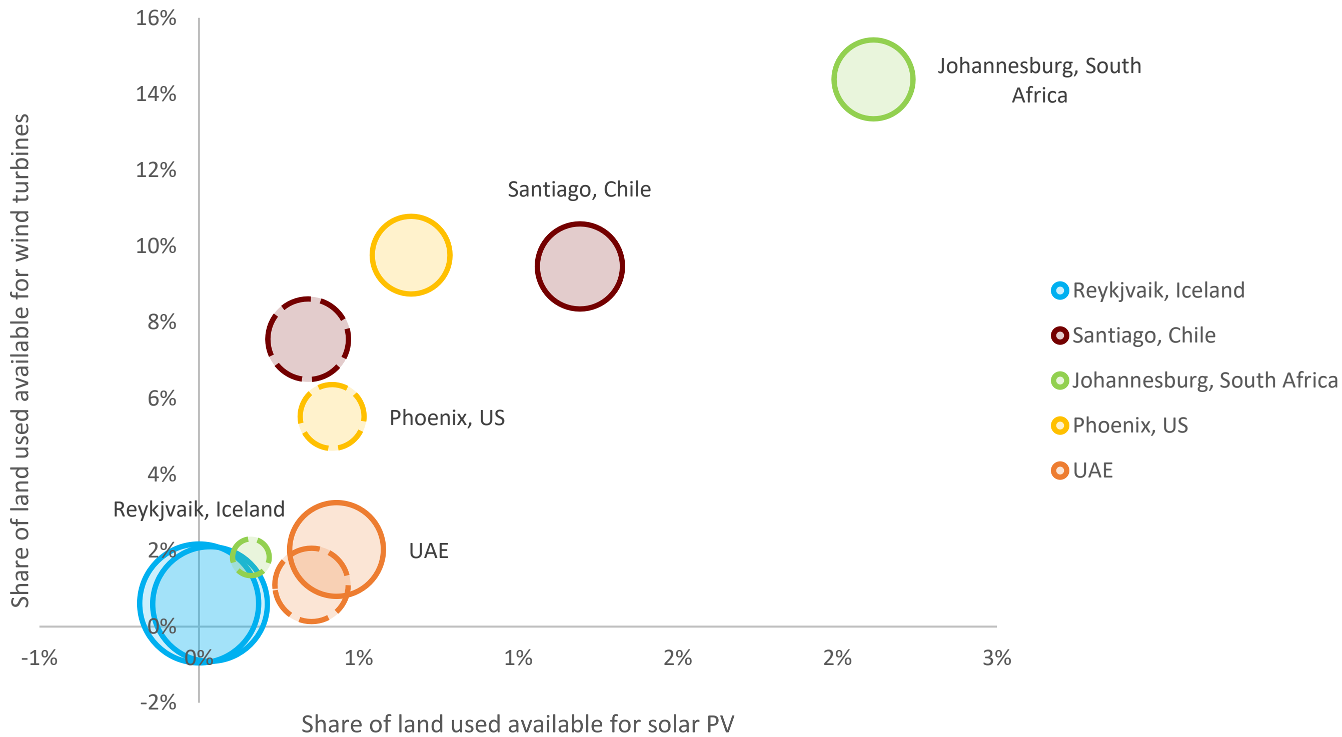

Supplementary Figure 15: Relative land use requirements of the CEA practices by the type of land available for either solar PV or wind turbines akin to Supplementary Figure 14, only showing the regions with a small required share of the available land for energy generation. The bubble size depicts the net land use per person subtracted with savings of co-locating solar PV and wind. The dashed-line circle is for greenhouses and the solid-line circle is for plant factories.

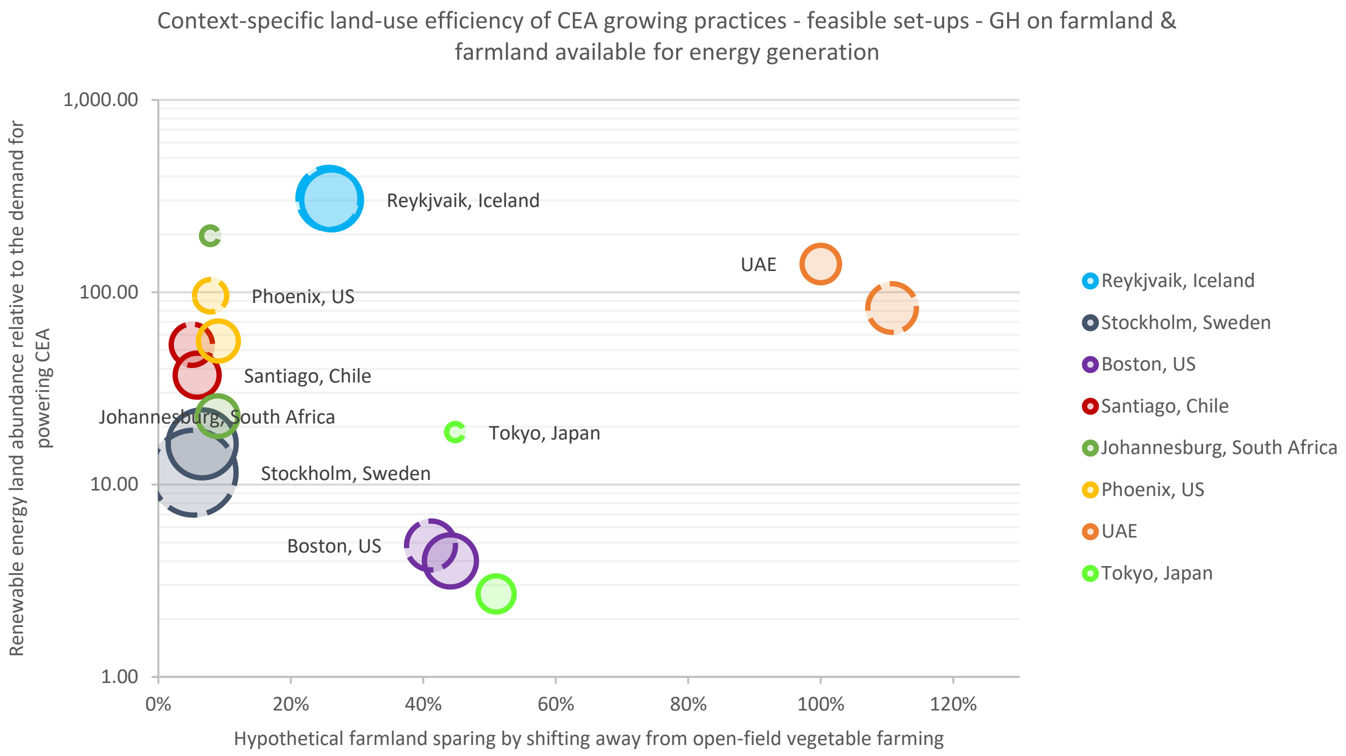

Supplementary Figure 16: Relative land use requirements of the CEA practices akin to Figure 5 in the main text. Farmland was considered partly suitable for renewable energy generation. The bubble size depicts the net land use per person subtracted with savings of co-locating solar PV and wind. The dashed-line circle is for greenhouses and the solid-line circle is for plant factories.

References

1. Weidner, T., Yang, A. & Hamm, M. W. Energy optimisation of plant factories and greenhouses for different climatic conditions. *Energy Convers. Manag.* **243**, 114336 (2021).

2. Sokolow, J., Kennedy, G. & Attwood, S. Managing Crop tradeoffs: A methodology for comparing the water footprint and nutrient density of crops for food system sustainability. *J. Clean. Prod.* **225**, 913–927 (2019).

3. Deng, Y. Y. *et al.* Quantifying a realistic, worldwide wind and solar electricity supply. *Glob. Environ. Chang.* **31**, 239–252 (2015).

4. Zappa, W. & van den Broek, M. Analysing the potential of integrating wind and solar power in Europe using spatial optimisation under various scenarios. *Renew. Sustain. Energy Rev.* **94**, 1192–1216 (2018).

5. Hoogwijk, M., de Vries, B. & Turkenburg, W. Assessment of the global and regional geographical, technical and economic potential of onshore wind energy. *Energy Econ.* **26**, 889–919 (2004).

6. Domínguez Bravo, J., García Casals, X. & Pinedo Pascua, I. GIS approach to the definition of capacity and generation ceilings of renewable energy technologies. *Energy Policy* **35**, 4879–4892 (2007).

7. Lopez, A., Roberts, B., Heimiller, D., Blair, N. & Porro, G. U.S. Renewable Energy Technical Potentials: A GIS-Based Analysis. *Natl. Renew. Energy Lab. Doc.* **1**, 1–40 (2012).

8. Hoefnagels, R. *et al. Long Term Potentials and Costs of RES Part I: Potentials, Diffusion and Technological learning*. www.reshaping-res-policy.eu (2011).

9. Wang, Q., M'Ikiugu, M. M. & Kinoshita, I. A GIS-based approach in support of spatial planning for renewable energy: A case study of Fukushima, Japan. *Sustain.* **6**, 2087–2117 (2014).

10. Miskin, C. K. *et al.* Sustainable co-production of food and solar power to relax land-use constraints. *Nat. Sustain.* **2**, 972–980 (2019).

11. Yue, C. D. & Wang, S. S. GIS-based evaluation of multifarious local renewable energy sources: A case study of the Chigu area of southwestern Taiwan. *Energy Policy* **34**, 730–742 (2006).

12. Archontoulis, S. V. *et al.* Predicting crop yields and soil-plant nitrogen dynamics in the US Corn Belt. *Crop Sci.* **60**, 721–738 (2020).

13. Qadir, G. & Malik, M. A. Growing degree days and yield relationship in sunflower (Helianthus annuus L.). *Int. J. Agric. Biol.* (2007).

14. Ramankutty, N., Foley, J. A., Norman, J. & McSweeney, K. The Global Distribution of Cultivable Lands : Current Patterns and Sensitivity to Possible Climate Change. *Glob. Ecol. Biogeogr.* **11**, 377–392 (2002).

15. Vogel, E. *et al.* The effects of climate extremes on global agricultural yields. *Environ. Res. Lett.* **14**, (2019).

16. Wang, E. & Engel, T. Simulation of phenological development of wheat crops. *Agric. Syst.* **58**, 1–24 (1998).

17. Aslam, M. A. *et al.* Can growing degree days and photoperiod predict spring wheat phenology? *Front. Environ. Sci.* **5**, 1–10 (2017).

18. Li, L., Li, X., Chong, C., Wang, C. H. & Wang, X. A decision support framework for the design and operation of sustainable urban farming systems. *J. Clean. Prod.* **268**, 121928 (2020).

19. Singh, S. Agrometeorological Requirements for Sustainable Vegetable Crops Production. *J. Food Prot.* **2**, 1–22 (2018).

20. Parthasarathi, T., Velu, G. & Jeyakumar, P. Impact of Crop Heat Units on Growth and Developmental Physiology of Future Crop Production: A Review. *Res. Rev. J. Crop Sci. Technol.* **2**, 11–18 (2013).

21. Benis, K., Reinhart, C. & Ferrão, P. Development of a simulation-based decision support workflow for the implementation of Building-Integrated Agriculture (BIA) in urban contexts. *J. Clean. Prod.* **147**, 589–602 (2017).

22. Fick, S. E. & Hijmans, R. J. WorldClim 2: new 1-km spatial resolution climate surfaces for global land areas. *Int. J. Climatol.* **37**, 4302–4315 (2017).

23. Rosenzweig, C., Tubiello, F. N., Goldberg, R., Mills, E. & Bloomfield, J. Increased crop damage in the US from excess precipitation under climate change. *Glob. Environ. Chang.* **12**, 197–202 (2002).

24. Martinez-Feria, R. A. & Basso, B. Unstable crop yields reveal opportunities for site-specific adaptations to climate variability. *Sci. Rep.* **10**, 1–10 (2020).

25. Biswas, S. C. Vegetable cultivation in the monsoon season in Bangladesh Vegetable cultivation in the monsoon season in Bangladesh. (2016) doi:10.13140/RG.2.1.1226.5209.

26. Hazra, P. Upgradation of the vegetable production scenario of Bangladesh: suggested strategy. *J. Agrofor. Env.* **2**, 201–204 (2008).

27. Li, Y., Guan, K., Schnitkey, G. D., DeLucia, E. & Peng, B. Excessive rainfall leads to maize yield loss of a comparable magnitude to extreme drought in the United States. *Glob. Chang. Biol.* **25**, 2325–2337 (2019).

28. FAO. *Damage and losses from climate-related disasters in agricultural sectors*. www.fao.org/3/a-i5128e.pdf.

29. Feng, S. & Hao, Z. Quantifying likelihoods of extreme occurrences causing maize yield reduction at the global scale. *Sci. Total Environ.* **704**, 135250 (2020).

30. Oyekale, J., Petrollese, M., Tola, V. & Cau, G. Impacts of renewable energy resources on effectiveness of grid-integrated systems: Succinct review of current challenges and potential solution strategies. *Energies* **13**, (2020).

31. Laugs, G. A. H., Benders, R. M. J. & Moll, H. C. Balancing responsibilities: Effects of growth of variable renewable energy, storage, and undue grid interaction. *Energy Policy* **139**, 111203 (2020).

32. Kapica, J. Wind and photovoltaic potential in Europe in the context of mid-term energy storage. *J. Renew.*

Sustain. Energy **12**, 034101 (2020).

33. Dujardin, J., Kahl, A., Kruyt, B., Bartlett, S. & Lehning, M. Interplay between photovoltaic, wind energy and storage hydropower in a fully renewable Switzerland. *Energy* **135**, 513–525 (2017).

34. Johlas, H., Witherby, S. & Doyle, J. R. Storage requirements for high grid penetration of wind and solar power for the MISO region of North America: A case study. *Renew. Energy* **146**, 1315–1324 (2020).

35. Moore, N. Large Scale Grid Integration of Wind and Solar Power with Storage. *Macalester J. Phys. Astron.* **8**, 13 (2020).

36. Putnam, M. & Perez, M. *Solar Potential Analysis Report*. *MN Solar Pathways* https://energy.gov/solar-office. (2018).

37. Perez, M., Perez, R., Rábago, K. R. & Putnam, M. Overbuilding & curtailment: The cost-effective enablers of firm PV generation. *Sol. Energy* **180**, 412–422 (2019).

38. Saunders, P. J. *Land Use Requirements of Solar and Wind Power Generation: Understanding a Decade of Academic Research ENERGY INNOVATION REFORM PROJECT*. (2020).

39. Denholm, P., Hand, M., Jackson, M. & Ong, S. Land Use Requirements of Modern Wind Power Plants in the United States. *Natl. Renew. Energy Lab.* **Technical**, 46 (2009).

40. McDonald, R. I., Fargione, J., Kiesecker, J., Miller, W. M. & Powell, J. Energy sprawl or energy efficiency: Climate policy impacts on natural habitat for the United States of America. *PLoS One* **4**, (2009).

41. McGowan, J. G. & Connors, S. R. Windpower: A turn of the century review. *Annu. Rev. Energy Environ.* **25**, 147–197 (2000).

42. MacKay, D. J. C. Solar energy in the context of energy use, energy transportation and energy storage. *Philos. Trans. R. Soc. A Math. Phys. Eng. Sci.* **371**, 20110431 (2013).

43. IRENA. *Future of solar Photovoltaic*. *International Renewable Energy Agency (IRENA)* (2019).

44. Bloomberg. *New Energy Outlook 2019*. (2019).

45. Fu, R., Feldman, D. & Margolis, R. *U.S. Solar Photovoltaic System Cost Benchmark: Q1 2018*. www.nrel.gov/publications. (2009).

46. Milborrow, D. Energy cost analysis 2020: Wind is ready for zero-subsidy future. https://www.windpowermonthly.com/article/1671659/energy-cost-analysis-2020-wind-ready-zero-subsidy-future (2020).

47. Orrell, A., Preziuso, D., Foster, N., Morris, S. & Homer, J. *2018 Distributed Wind Market Report*. http://www.ntis.gov/about/form.aspx.

48. IRENA. *Technology Beif: Biogas for Road Vehicles*. (2018).

49. World Nuclear Association. Carbon Dioxide Emissions From Electricity. https://www.world-nuclear.org/information-library/energy-and-the-environment/carbon-dioxide-emissions-from-electricity.aspx.

50. OR Reykjavik Energy. E2 Emission Intensity. https://annualreport2020.or.is/climate-issues/e2-emission-intensity/.

51. carbonfootprint.com. International Electricity Factors. https://www.carbonfootprint.com/international_electricity_factors.html.

52. Ritchie, H. & Roser, M. CO_2 and Greenhouse Gas Emissions. *Our World in Data* https://ourworldindata.org/co2-and-other-greenhouse-gas-emissions (2020).